Biol. Stud. 2025, 19(3), 33–54 • doi: https://doi.org/10.30970/sbi.1903.844
www.http://publications.lnu.edu.ua/journals/index.php/biology

UDC: 577.33

IMPACT OF Fe_3O_4 NANOPARTICLES *IN VITRO* ON THE CONTRACTILE ACTIVITY OF SMOOTH MUSCLES OF RAT *ANTRUM* AND AORTA

Yuliia Podhaietska [1], ***Sergiy Kolotilov*** [2], ***Mykyta Ivanytsya*** [2,4], ***Diana Doronina*** [2,4], ***Anna Velbovets*** [4], ***Oleksandr Chunikhin*** [3], ***Oksana Malanchuk*** [5], ***Ivan Voiteshenko*** [1], ***Olga Tsymbalyuk*** [1]

[1] *Taras Shevchenko National University of Kyiv, 64 Volodymyrska St., Kyiv 01601, Ukraine*

[2] *L. V. Pisarzhevsky Institute of Physical Chemistry, the NAS of Ukraine 31 Nauky Ave., Kyiv, 03028, Ukraine*

[3] *O. V. Palladin Institute of Biochemistry, the NAS of Ukraine 9 Leontovycha St., Kyiv 01601, Ukraine*

[4] *Enamine Ltd., 78 Winston Churchill St., 02094 Kyiv, Ukraine*

[5] *Danylo Halytskyi Lviv National Medical University, 69, Pekarska St., Lviv 79010, Ukraine*

Podhayetska, Yu., Kolotilov, S., Ivanytsya, M., Doronina, D., Velbovets, A., Chunikhin, O., Malanchuk, O., Voiteshenko, I., & Tsymbalyuk, O. (2025). Impact of Fe_3O_4 nanoparticles *in vitro* on the contractile activity of smooth muscles of rat *antrum* and aorta. *Studia Biologica*, 19(3), 33–54. doi:10.30970/sbi.1903.844

Background. Magnetic iron oxide nanoparticles are among the most promising materials for creating new theranostics tools for malignant neoplasms. Currently, a number of medical preparations based on iron oxide nanoparticles have been introduced into diagnostic and medical practice, MRI diagnostics, and photosensitizing therapy, as well as a source of iron for patients with a deficiency of this element. However, these nanoparticles are not completely neutral with respect to the functions of organs and tissues of the body, in particular the cardiovascular, respiratory, genitourinary, and central nervous systems. The effect of Fe_3O_4 nanoparticles on the contraction of smooth muscles of the gastrointestinal tract and aorta has not been studied. The purpose of our study was to clarify the features and mechanisms of the *in vitro* effect of these nanoparticles on the functional activity of the annular smooth muscles of the stomach and preparations of rat aortic rings.

Materials and Methods. A suspension of Fe_3O_4 nanoparticles in water was used. The nanoparticles were characterized by transmission electron microscopy (TEM)

and selected area electron diffraction (SAED). The average hydrodynamic diameter of Fe_3O_4 nanoparticles in suspension upon stabilization with oleic acid (1%), bovine serum albumin (7.5%), and DMSO (1%) was determined by dynamic light scattering.

The tenzometric experiments were conducted in the isometric recording mode on isolated preparations of circular smooth muscles of the *antrum* and rings of the thoracic aorta of rats. In the case of *antrum* muscles, contractions were induced by application of a high-potassium solution (80 mM), acetylcholine (10^{-5} M), and nicotine (10^{-4} M), and in the case of aortic preparations – a high-potassium solution (80 mM) and epinephrine (10^{-6} M). Contractions were analyzed by mechanokinetic analysis methods.

Results. It was determined that under the conditions of using DMSO as a stabilizer, the suspension contained a minimal quantity of aggregates of Fe_3O_4 nanoparticles, showing a peak with an average value of 67.2 nm and a width of 75.3 nm (in terms of number), and was quite stable.

It was found that the use of Fe_3O_4 (10^{-4} mg/mL) *in vitro* led to the activation of contractions of smooth muscle preparations of the stomach and aorta caused by the application of a high-potassium solution. Also, under the action of Fe_3O_4, reversible activation of spontaneous contractions of the smooth muscle of the stomach was observed. Mechanokinetic analysis has established that Fe_3O_4 caused an increase in force, time, and impulse parameters.

It was found that under the action of Fe_3O_4 nanoparticles, epinephrine-activated contractions of aortic rings and nicotine-activated contractions of stomach preparations were significantly reduced. However, Fe_3O_4 caused a significant increase in acetylcholine-activated contractions of gastric preparations.

Conclusions. Fe_3O_4 nanoparticles modulate spontaneous and induced contractions of the *antrum* and aortic smooth muscle preparations. The main mechanisms of such modulation likely involve the activation of voltage-gated Ca^{2+} ion influx into smooth muscle cells and the sorption of epinephrine and nicotine by these nanoparticles.

Keywords: aorta, antral stomach, Fe_3O_4 nanoparticles, voltage-gated Ca^{2+}-channels, acetylcholine, epinephrine, nicotine, mechanokinetic parameters

INTRODUCTION

Among modern approaches to creating novel medications to combat cancer, the development of means combining the properties of preparations that are simultaneously suitable for both diagnostics and therapy – theranostics – is gaining momentum (Salimi *et al*., 2022; Al-Thani *et al*., 2024). The optimal means of theranostics must be able to accumulate in a malignant formation with significantly greater selectivity compared to healthy tissues. This selective accumulation may occur due to functional groups in their structure, which bind ligands that are expressed in tumor cells and capable of forming covalent or non-covalent interactions with the latter. It is also likely that the physicochemical properties of nanoparticles allow them to remain in the alkalized medium of the neoplasm more effectively. As a result, the theranostics means improve the neoplasm visualization (using the methods of magnetic resonance imaging (MRI), computer tomography (CT), ultrasound (US) scanning, etc.) and enable precision treatment by novel methods: photothermal and photodynamic therapy, targeted delivery of medical substances and their controlled release, as well as tracing the distribution of cells during cell therapy (Babsky *et al*., 2025; Zhao *et al*., 2020; Finiuk *et al*., 2021; Nowak-Jary & Machnicka, 2024).

Nanosized materials appear to be the promising foundation for the creation of theranostic means; thus, in recent decades, nanomedicine has been singled out as a novel branch of pharmacology. In particular, superparamagnetic nanostructures based on iron, cobalt, and nickel are regarded as the basis for biomedical diagnostics, induced hyperthermia, magnetic cell separation, and the delivery of medical agents (Vallabani & Singh, 2018).

Among nanosized materials, some of the most promising means of theranostics include superparamagnetic iron oxide nanoparticles (Fe_3O_4 magnetite, α-Fe_2O_3 hematite, ɣ-Fe_2O_3 maghemite, and β-Fe_2O_3). Currently, there are magnetite-based preparations approved by the FDA, including GastroMARK, Umirem, Feridex, Endorem, Feraheme, Feridex IVR, and Gastromark. Additionally, several preparations are undergoing clinical trials (Vakili-Ghartavol *et al*., 2020; Nowak-Jary & Machnicka, 2024). The aforementioned preparations are utilized in MRI diagnostics, multimodal visualization, magnetic hyperthermia, and photosensitive therapy due to the properties of enzymes (peroxidase activity) and their ability to deliver the preparations for pharmacotherapy and hemotherapy selectively into the tissues (Vallabani & Singh, 2018; Zhao *et al*., 2020; Mehta, 2022). For instance, Fe_3O_4 nanoparticles can act as ultrasensitive contrasting substances for early detection of solid tumors (from 1 mm in diameter) using the MRI in the modes of T1- and T2-weighted imaging (depending on the size of particles) and possess improved biocompatibility compared to Gd^{3+}-containing preparations (Jia *et al*., 2016; Zhao *et al*., 2020). In combination with other nanoparticles, proteins, and dyes, the nanoparticles of iron oxide are considered suitable nanocomplexes to be used in laboratory medical diagnostics in case of simultaneous MRI and CT (a complex of nanoparticles of gold and magnetite), and three-mode imaging using the methods of MRI, positron-emission tomography (PET), and visualization in near infrared fluorescent range (NIRF) (Vallabani & Singh, 2018). In 2015, Ferumoxytol (Feraheme), a preparation based on magnetic nanoparticles of magnetite, coated with polyglucose sorbitol carboxymethyl ether, was approved by the FDA (US Food and Drug Administration) for treatment of patients with iron deficiency and chronic renal disease (Castaneda *et al*., 2011; Vallabani & Singh, 2018). The development of theranostic preparations based on iron oxide nanoparticles is a highly promising and strategically important direction in modern biology and medicine (Younis *et al*., 2022; Singh *et al*., 2024; Benjamin & Nayak, 2025).

However, their potential side effects pose serious concerns regarding the medical application of nanosized materials. The properties of nanoparticles that make them more advantageous compared to larger particles (a high ratio between surface area and volume, and high uncompensated superficial energy) are responsible for their potential toxicity in living organisms (Younis *et al*., 2022; Shoudho *et al*., 2024). On the other hand, the prooxidant properties of nanoparticles depend on their chemical composition and charge, surface area, method of synthesis, reactivity, presence of a coating, and composition (Nowak-Jary & Machnicka, 2024). A considerable amount of information regarding the impact of iron oxide nanoparticles on living systems has already been accumulated. On the one hand, due to their unique physical and chemical properties, iron oxide nanoparticles of small diameter, as well as other nanoparticles, induce the formation of reactive oxygen intermediates, free radical processes, and oxidative stress in cells (Driscoll *et al*., 2021; Joudeh & Linke, 2022; Baabu *et al*., 2022; Wu *et al*., 2022; Nowak-Jary & Machnicka, 2024). On the other hand, most *in vitro* and *in vivo* studies have not detected any toxicity of iron oxide nanoparticles in doses under 100 μg/mL (Vakili-Ghartavol *et al*., 2020). For instance, non-coated nanoparticles of Fe_3O_4 in concentrations up to

100 μg/mL had no cytotoxic effect on the cells of human hepatocarcinoma (Gholami *et al*., 2015). On the contrary, in some investigations, toxic effects at the impact of iron oxide nanoparticles were shown in the following concentrations: above 2 μg/mL (Shukla *et al*., 2014), above 3.25 μg/mL (Feng *et al*., 2018), above 6.25 μg/mL (Obireddy & Lai, 2022), 25 μg/mL (Hilger *et al*., 2003), and <100 μg/mL (Zhang *et al*., 2021). Therefore, the inspection for toxicity and biocompatibility is one of the foremost tasks when investigating potential means to be used in theranostics.

Despite a large array of information about the regularities and mechanisms of the effect of iron oxide nanoparticles on the organs and tissues of the respiratory, genitourinary and central nervous systems, liver, and heart (Nowak-Jary & Machnicka, 2024), there are almost no data regarding possible effects of these nanoparticles on the function of smooth muscles of the digestive tract and insufficient information about vessels. For instance, the study of Rivière has not detected the effect of Fe_3O_4 and γ-Fe_2O_3 nanoparticles in concentrations between 0.1 and 10.0 mmol/L of iron on the survival of smooth muscle cells (Rivière *et al*., 2005). Also, against the background of the internalization of magnetic nanoparticles of iron oxide, extremely peculiar effects on the change in the expression of actin and calponin genes, without any changes in cell morphology, proliferation, or metabolic activity, were found (Angelopoulos *et al*., 2016). Assessment of nanoparticles' action on smooth muscles may be carried out by measuring their contractile functions. The model of cellular spheroids from smooth muscle cells of the aorta was used to determine an increase in collagen formation and a decrease in contractility under the impact of iron oxide nanoparticles (Olsen *et al*., 2015). The study of S. Líšková revealed that the application of Fe_3O_4 (1 mg Fe/kg intravenously) to rats resulted in an increase in components of acetylcholine-induced relaxation of femoral arteries, which is sensitive to blocking of nitrogen oxide synthases, and a decrease in their sensitivity to sodium nitroprusside, a donor for nitrogen oxide (Líšková *et al*., 2020). The only investigation related to checking the effect of Fe_3O_4 nanoparticles (50–100 nm) on the contractile function of vessels *in vitro* was conducted using endothelium-containing and endothelium-denuded preparations of human mesenteric arteries (Vukova *et al*., 2016). Under conditions of preliminary incubation for 10 min with cumulative increasing concentrations of nanoparticles from 0.023 to 2.31 μg/μL, no effects on contractions, induced by high-potassium solution and endothelin 1, were found.

Considering the lack of up-to-date information regarding the effect of Fe_3O_4 nanoparticles on the contraction of smooth muscles of the gastric tract and the aorta, the aim of our investigation was to find out the regularities and predict the mechanisms of the *in vitro* effect of these nanoparticles on the functional activity of circular smooth muscles of the *antrum* and preparations of the rings of the rat aorta.

MATERIALS AND METHODS

Synthesis of Fe_3O_4 nanoparticles. Fe_3O_4 nanoparticles were synthesized by a slight modification of the reported procedure (Giri *et al*., 2005).

The solution of KOH (12.5 g, 220 mmol, 24 equiv.) in 100 mL of water was heated to 90 °C in an oil bath. Then the solution, containing $FeSO_4 \cdot 7H_2O$ (2.5 g, 9 mmol, 1 equiv.) and $FeCl_3 \cdot 6H_2O$ (4.9 g, 18 mmol, 2 equiv.) in 150 mL of water, was added dropwise. The reaction mixture was further kept at 90 °C for 1 h, then allowed to cool down to room temperature. The solid Fe_3O_3 nanoparticles were separated from the solution containing KOH and other salts by decantation, and were washed out by repeated additions of por-

tions of distilled water and decantation until the pH of the solution was slightly below 7 (corresponding to the pH of distilled water). Then the volume of the Fe_3O_4 suspension was adjusted to 200 mL. The resulting suspension contained 10 mg of Fe_3O_4 per 1 mL.

TEM and SAED measurements. The TEM and SAED measurements were performed using a PEM-125K transmission electron microscope (Selmi Ltd., Sumy, Ukraine) operating at a 100 kV acceleration voltage. The sample was deposited on a copper grid, covered with a thin film of amorphous carbon, as reported by (Subotin *et al*., 2023).

Determining the hydrated diameters of Fe_3O_4 nanoparticles by the method of dynamic light scattering. To study the hydrodynamic diameter, the suspensions of Fe_3O_4 nanoparticles in the doubly distilled water were stabilized by the addition of oleic acid (1%), bovine serum albumin (BSA, the concentration in the stock solution of 7.5%) and DMSO (the concentration in the stock solution of 1%), mixed using the Wortex mechanical homogenizer and processed with ultrasound for 5 min.

The average hydrodynamic diameter of Fe_3O_4 nanoparticles in aqueous suspensions was determined by the method of dynamic light scattering using ZetaSizer-3 laser correlation spectrometer (Malvern Instruments, Great Britain). This device was equipped with a He-Ne laser LGN-111 (P = 25 mWt, λ = 633 nm) and had a working measuring range from 1 nm to 20 μm. The laser irradiation, scattered from the suspension of nanoparticles, was registered in 5 repeated sessions (1 min each) at 22 °C under a dissipation angle of 90 °C. The primary processing of experimental data was performed using the servicing software PCS-Size mode v1.61.

Tenzometric studies. The study was conducted using Wistar line rats from the population of the vivarium in the Taras Shevchenko National University of Kyiv. The animals were kept on a standard diet and under standard vivarium conditions: temperature of 20±2 °C, relative air humidity of 50–70 %, light regime – light:darkness = 12:12 h. All the manipulations with the animals were conducted according to the International Convention for the Protection of Animals and the Law of Ukraine “On Protection of Animals from Cruelty” (the Minutes of the Bioethics Commission of the Taras Shevchenko National University of Kyiv No.8 dated December 26, 2024). The rats were euthanized by hypoxia, induced by carbon dioxide (CO_2).

The tenzometric experiments were conducted in the isometric mode using preparations of stripes, free from the mucous membrane (1.5×10 mm), of circular smooth muscles of the *antrum* and the circles (2–3 mm wide) of the thoracic aorta with preserved endothelium. The smooth muscle preparations were placed into the working chamber (the efficient volume of 2 mL) with the flowing Krebs solution (the flow rate of 8 mL/min), thermostated at 37 °C. The preparations were provided with passive tension at the rate of 10 mN and left for at least 1 h. The signals were registered after being enhanced using the analogue-to-digital transformer.

Krebs solution was used in the experiments (mM): 120.4 NaCl; 5.9 KCl; 15.5 $NaHCO_3$; 1.2 NaH_2PO_4; 1.2 $MgCl_2$; 2.5 $CaCl_2$; 11.5 glucose; pH of the solution was 7.4. The high-potassium solution (HPS with the concentration of K^+ ions of 80 mM) was used in experiments. It was prepared by isotonic replacement of some Na^+ ions in the initial Krebs with an equimolar amount of K^+ ions. In addition, the work involved agonists (all produced by “Sigma”): muscarinic cholinoreceptors, acetylcholine (10 μM), adrenoreceptors, epinephrine (at a concentration of 1 μM, at which beta-adrenergic receptors are activated to a greater extent (Yang *et al*., 2021)), and nicotine cholinoreceptors, nicotine (100 μM).

Since the method of dynamic light scattering was used to determine that the most optimal properties (dispersion of nanoparticle sizes in suspension and its stability) of the suspension of Fe_3O_4 nanoparticles were obtained using DMSO, it was used in the studies of the contractile activity of muscle preparations, and all the tenzometric experiments were conducted against the background of 0.1% DMSO solution.

Mechanokinetic analysis. The spontaneous contractions of the *antrum* preparations were analyzed using the multiparameter mechanokinetic analysis (Kosterin *et al*., 2021). According to this method, the following groups of parameters were calculated: time (τ_0 – time, during which the contraction amplitude is achieved; characteristic values of time for contraction and relaxation phases, in which maximal velocities are achieved, τ_C and τ_R, respectively), force (F_{max} – contraction amplitude; force parameters in phases of contraction and relaxation, when the maximal velocity is observed, F_C and F_R, respectively), velocity (maximal velocities of contraction and relaxation phases, V_C and V_R, respectively) and impulse (I_{max} – force impulse, observed in the amplitude point; force impulse parameters in contraction and relaxation phases, when maximal velocity is observed, I_C and I_R, respectively).

The contractions, induced by the application of the high-potassium solution and an agonist, were impacted by Kosterin–Burdyga's method of kinetic analysis (Burdyga & Kosterin, 1991), used to assess the maximal velocities of the phases of contraction (V_{nc}) and relaxation (V_{nr}), normalized with consideration of the amplitude.

Statistical analysis. The experimental data were processed by variation statistics methods using OriginPro 2018 software. The samplings for normality were checked using the Shapiro–Wilk test. The paired version of Student's *t*-test was used to determine the reliable differences between the mean values of the samplings. The results were considered reliable on condition of the probability value $p < 0.05$. The validation analysis of chart data approximation by the linear function, while using the mechanokinetic analysis, was performed using Fisher's criterion; determination coefficients (R^2) were at least 0.96 in all cases. The results were presented as the mean ± standard error of the mean value, n – the number of experiments.

RESULTS AND DISCUSSION

TEM and SAED studies of Fe_3O_4 nanoparticles. The Fe_3O_4 nanoparticles had quite uniform size, as revealed by TEM (**Fig. 1*A***). All particles were in the range of 12–18 nm, with an average size of approximately 15 nm. Notably, no particles smaller than 9–10 nm, as well as larger than 20 nm, were detected. Crystallinity of Fe_3O_4 nanoparticles was confirmed by SAED pattern (**Fig. 1*B***). Concentric circles, typical for nanosized crystals, were observed; the positions of circles were consistent with those expected for cubic spinel Fe_3O_4 phase. No separate distinct reflections were observed, confirming the absence of crystallites larger than 25–30 nm.

Determining the sizes of Fe_3O_4 nanoparticles in suspensions by the method of dynamic light scattering. Taking into account the known tendency of ehe magnetic Fe_3O_4 nanoparticles to aggregate in aqueous solutions, we performed the measurements under conditions of stabilizing the suspension. Since the oleic acid, bovine serum albumin (BSA), and dimethylsulfoxide (DMSO) were used as stabilizers for their aqueous suspensions in several studies on the biomedical application of iron oxide nanoparticles

(Yan *et al*., 2018; Yang *et al*., 2015; Yotsomnuk *et al*., 2025), the hydrodynamic diameters of Fe_3O_4 nanoparticles were estimated upon suspending in the presence of these substances. While suspended in the bidistillate, Fe_3O_4 nanoparticles were characterized by rather wide margins of the distribution of hydrodynamic diameter indices. For instance, in terms of intensity, their distribution was bimodal: the first peak (with the area of 1.5 % of the total) had an average value of 112 nm and a width of 72 nm; the second peak (with the area of 98.5 % of the total) had an average value of 2673 nm and a width of 4322 nm. The distribution of hydrodynamic diameters of nanoparticles in terms of volume was characterized by one peak with an average value of 3863 nm and a width of 3303 nm. Finally, the distribution of hydrodynamic diameters of Fe_3O_4 nanoparticles in terms of number was as follows: an average value of 50 nm and the width of the peak of 39 nm (the largest number had the size of 43 nm); also, the suspension was not stable (**Fig. 2*A***).

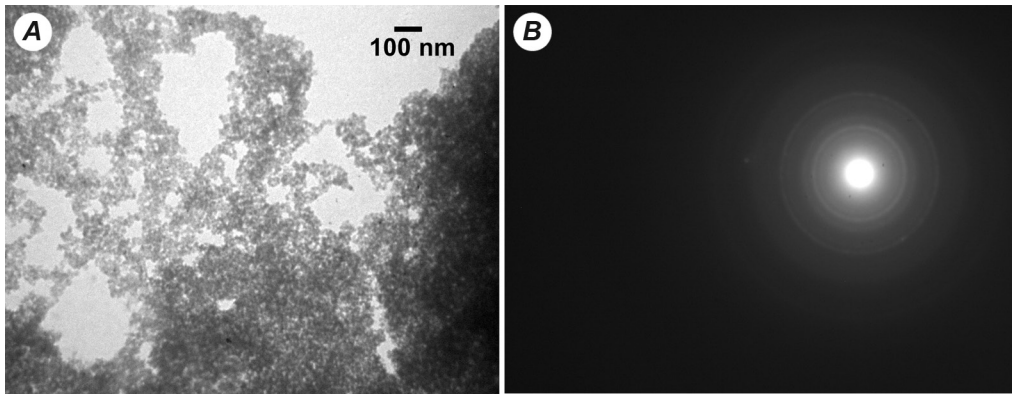

Fig. 1. TEM image (***A***) and SAED pattern (***B***) for Fe_3O_4 nanoparticles

In the case of treating the aqueous suspension with ultrasound, its characteristics practically did not improve. The distribution of sizes of nanoparticles in terms of intensity was characterized by one peak with an average value of 4360 nm and a width of 6990 nm. The distribution of hydrodynamic diameters of nanoparticles in the suspension in terms of volume was characterized by an average value of 5646 nm and the width of the peak of 5736 nm. The distribution of hydrodynamic diameters of particles in terms of their number had an average value of 86 nm (the largest number of particles had an average size of 66 nm), and the width of the peak was 75 nm (**Fig. 2*A***). Similarly to the case without ultrasound treatment, the suspension of Fe_3O_4 particles was not stable.

The use of BSA to stabilize the suspension (with and without ultrasound treatment) could not be considered the optimal strategy either. Under these conditions, the hydrodynamic diameters of particles in the suspension were characterized by the distribution in terms of intensity with one peak, average values of which were 2535 nm and 2022 nm, and the width values of 2472 nm and 2923 nm, respectively, without and with ultrasound treatment. In both cases, the distribution of particles in terms of size had one peak with average values of 2837 nm and 2640 nm, and the peak width of 3811 nm and 2901 nm, respectively, without and with ultrasound treatment. Finally, the distribution of Fe_3O_4 agglomerates in terms of number without and with ultrasound treatment had one peak with the following parameters: maximum 2228 nm and 1219 nm, and the peak width of 2228 nm and 992 nm. (**Fig. 2*B***).

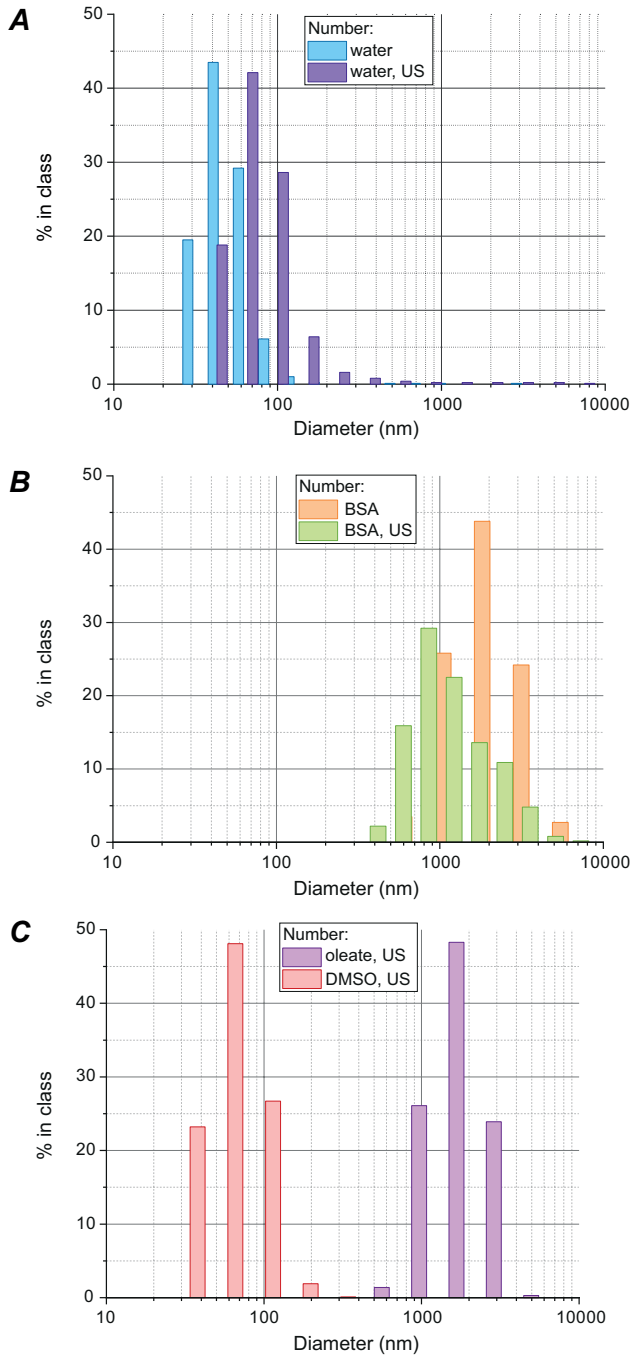

Fig. 2. The distribution of hydrodynamic diameters of Fe_3O_4 nanoparticles in terms of their number in suspensions: ***A*** – aqueous suspension without the stabilizer; not treated and treated with ultrasound (US); ***B*** – aqueous suspension; BSA is used as a stabilizer; not treated and treated with US; ***C*** – aqueous suspension; oleic acid and DMSO are used as stabilizers; treated with US. The summarized results of 5 registrations are presented

The application of oleic acid to stabilize the suspension of Fe_3O_4 particles was also accompanied by the formation of agglomerates of considerable size. Their distribution in terms of intensity was characterized by one peak with an average value of 1916 nm and a width of 1107 nm. The distribution in terms of volume had a peak with an average value of 2089 nm and a width of 2341 nm. The distribution of particles in terms of number was characterized by an average value of 1972 nm and the width of the peak of 2154 nm (**Fig**. **2*C***).

DMSO is the only organic solvent approved by the US Food and Drug Administration (FDA) for testing drug carriers (Capriotti & Capriotti, 2012; Ju-Nam *et al*., 2016); therefore, we used DMSO to prepare a suspension of Fe3O4 nanoparticles. The application of DMSO as a suspension stabilizer resulted in the widest range of the distribution of particles in terms of intensity (bimodal, with average values of 141 nm (3.3 % of the total intensity) and 33466 nm (96.7 % of the total intensity)) and volume (one peak with an average value of 15259 nm and a width of 16700 nm). However, under these conditions, we observed the most optimal distribution of particles in terms of their number: one peak with an average value of 67 nm and a width of 75 nm, where the highest number (48.1 %) of particles had an average size of 59 nm (**Fig. 2*C*).** These values are consistent with the results of particle size determination by TEM, considering that particles in suspension have large solvate shell. The suspension was rather stable under these conditions.

Therefore, in our further studies of contractile activity of smooth muscles, we used the stock solution of Fe_3O_4 nanoparticles in DMSO, which was introduced into working solutions under strict control to achieve a DMSO concentration of 0.1%. All tenzometric experiments were also conducted under the effect of 0.1% DMSO. It was previously determined that this DMSO concentration does not affect the functioning of smooth muscles (Ramnarine *et al*., 1994; Goud *et al*., 1998). Besides, another advantage of DMSO addition to the suspension is its ability to facilitate the penetration of medical preparations into tissues (Karim *et al*., 2023; Mashouf *et al*., 2024).

Basal tension and contractile activity of the preparations of rat aorta circles under the effect of Fe_3O_4 nanoparticles. When Fe_3O_4 nanomaterial penetrates inside an organism, it spreads with the blood, primarily affecting the vascular stream. Since, as stated above, the effects of these nanoparticles on the functioning of vascular smooth muscles were studied insufficiently, we investigated the *in vitro* impact of Fe_3O_4 on basal tension and contractile reactions of rat aorta, induced by the key pathways of excitation. We selected a concentration of nanoparticles of 10^{-4} mg/mL for our studies, as data from most investigations have demonstrated that this concentration is marginal in terms of inducing side effects on cell function (summarized in the review Nowak-Jary & Machnicka, 2024).

The addition of the suspension of Fe_3O_4 nanoparticles (10^{-4} mg/mL) to the solution, washing the muscle preparations, and preliminary incubation with them for 30 min did not change the basal tension of the preparations of rat aorta circles.

A convenient and adequate model to check the voltage-gated input of Ca^{2+} ions into myocytes is a contraction, activated by the high-potassium solution. In case of activating the contractions of aorta preparations by the application of the high-potassium solution (80 mM) against the background of Fe_3O_4 (10^{-4} mg/mL), we observed their considerable increase. For instance, the impact of nanoparticles resulted in an average amplitude of 176.3 ± 12.1% ($n = 5$, $p < 0.01$) compared to control values (**Fig. 3**).

Thus, due to the effect of Fe_3O_4 nanoparticles, there is an increase in voltage-gated input of Ca^{2+} ions to myocytes. This assumption is confirmed by the studies of

M. Yuan *et al*., in which the neurons of mesencephalon of mice were used to determine the ability of iron oxide nanoparticles to increase the input of Ca^{2+} ions via voltage-gated Ca^{2+}-channels of L-type (the authors assumed that it was due to the interaction between nanoparticles and the structures of the plasma membrane of cells) (Yuan *et al*., 2022).

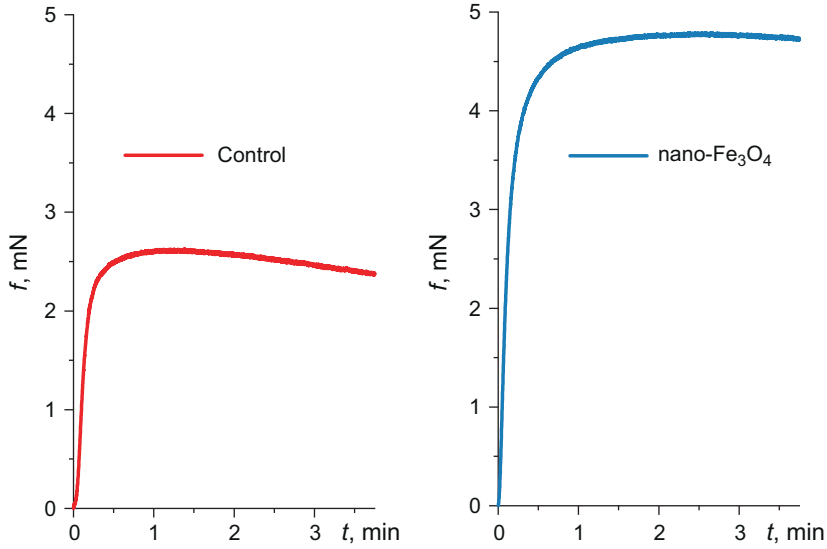

Fig. 3. The typical contractions of aorta ring preparations under activation with the high-potassium solution (80 mM) in control and under the effect of the suspension of Fe_3O_4 nanoparticles (the concentration of 10^{-4} mg/mL, the preliminary incubation lasted 30 min)

Contrary to the effect of activating the aorta contractions with the high-potassium solution, epinephrine-induced (10^{-6} M) contractions of preparations of aorta rings were inhibited after preliminary incubation with Fe_3O_4 nanoparticles. In this case, there was a considerable decrease in their amplitude (phase component, on average to 52.6±9.6 % regarding the control, n = 5, p <0.01), and the tonic component (on average to 46.3±8.1 % regarding the control, n = 5, p <0.01) (**Fig. 4**).

The mentioned effect of inhibiting epinephrine-activated contractions of aorta preparations may be related to the ability of Fe_3O_4 nanoparticles to sorb catecholamines selectively and with high affinity (Lin *et al*., 2013; Shi *et al*., 2022). Noteworthy is the effect of activating the fluctuations in the tension of the aorta wall, observed under the action of Fe_3O_4 nanoparticles (**Fig. 4**). Since Fe_3O_4 nanoparticles are known to affect the state of mechanosensitive ion channels, related to the regulation of the vascular wall tension, it may be assumed that it is their impact that causes an increase in epinephrine-induced fluctuations in the aorta ring tension (Wang *et al*., 2020).

Basal tension and spontaneous contractions of the circular smooth muscles of the rat *antrum* in the presence of Fe_3O_4 nanoparticles. We also studied the effects of Fe_3O_4 nanoparticles (10^{-4} mg/mL) *in vitro* on the functional activity of circular smooth muscles of the *antrum*. At first, the spontaneous contractile activity of the preparations was registered in control and against the background of the input of the suspension of Fe_3O_4 nanoparticles. The fixed concentration of nanoparticles of 10^{-4} mg/mL was selected for investigations.

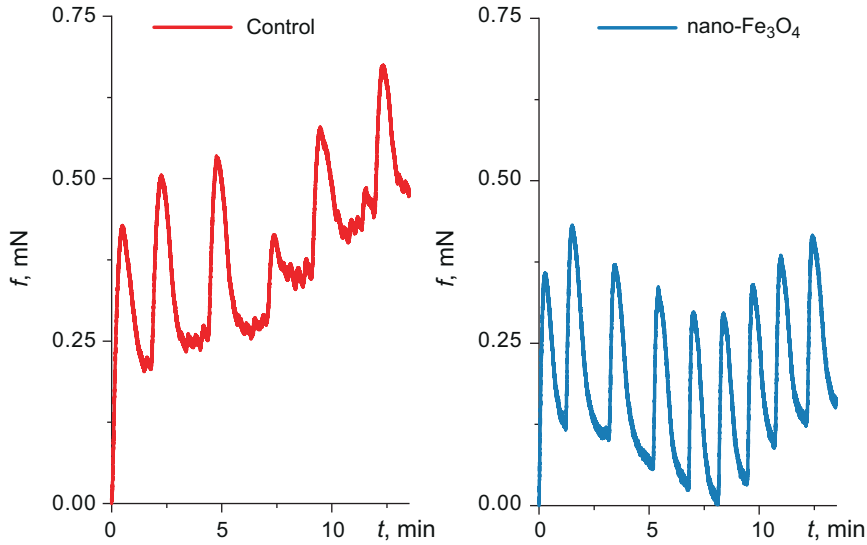

Fig. 4. Typical contractions of aorta ring preparations, induced by the application of epinephrine (10^{-6} M) in control and under the effect of Fe_3O_4 nanoparticles (the concentration of 10^{-4} mg/mL, the duration of the preliminary incubation of 30 min)

The addition of the suspension of Fe_3O_4 nanoparticles into the Krebs solution washing the smooth muscle preparations caused a considerable (on average by 53.1±6.3 % regarding the intact level) decrease in their basal tension, which reached a constant level on average 14.2±1.7 min after the beginning of the Fe_3O_4 application (**Fig. 5**). The mentioned effect was reversible, eliminated by washing with the normal Krebs solution.

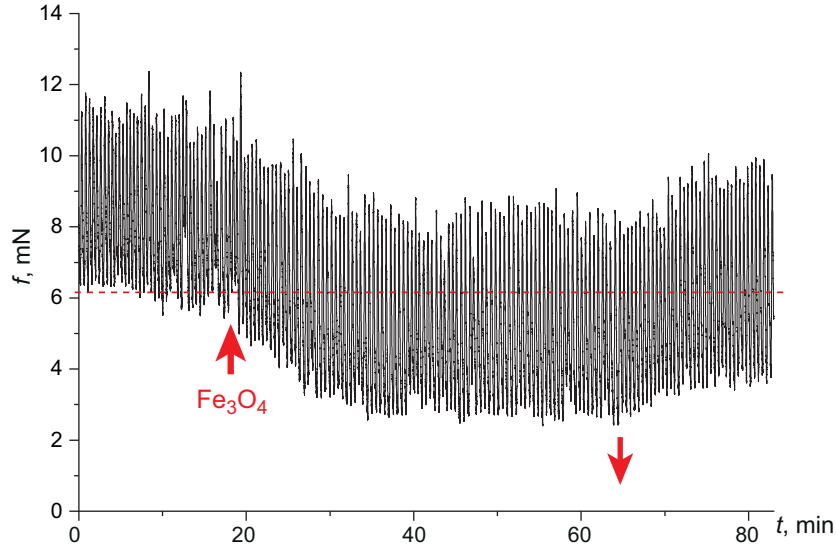

Fig. 5. The modulation of the basal tension and spontaneous contractions of circular smooth muscles of the rat *antrum* under the effect of the suspension of Fe_3O_4 nanoparticles (10^{-4} mg/mL). A typical mechanogram is presented

Under the effect of Fe_3O_4 nanoparticles, the frequency of spontaneous contractions remained unchanged (21.5±2.3 contractions in 10 min in control and 18.6±2.2 contractions in 10 min under the effect of Fe_3O_4). At the same time, the amplitude of spontaneous contractions increased on average to 115.6±2.4 % (n = 5, p <0.05) (**Fig. 6*A***).

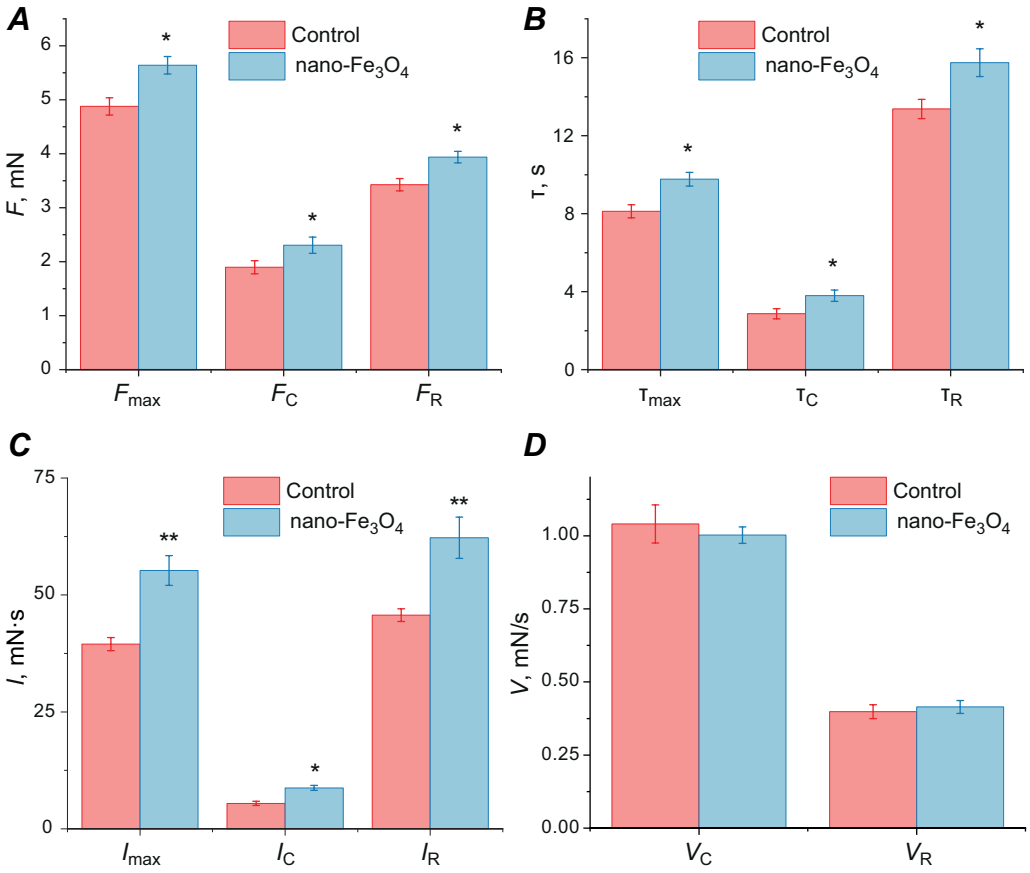

Fig. 6. The mechanokinetic parameters of spontaneous contractions of the circular smooth muscles of the rat *antrum* in control and under the effect of the suspension of Fe_3O_4 nanoparticles (10^{-4} mg/mL, the duration of the preliminary incubation of 30 min): ***A*** – force parameters (F_{max}, F_C and F_R); ***B*** – time parameters (τ_{max}, τ_C and τ_R); ***C*** – impulse parameters (I_{max}, I_C and I_R); ***D*** – velocity parameters (V_C and V_R). n = 5, * – p <0.05 and ** – p <0.01 – significant regarding the control parameter

Since the frequency of spontaneous contractions of smooth muscles of the gastrointestinal tract is conditioned by the pacemaker activity of interstitial cells of Cajal (Wang *et al*., 2025), and their amplitude depends on the level of free Ca^{2+} in myocytes during excitation (Yoneda *et al*., 2004), we can assume that Fe_3O_4 nanoparticles mostly affect the processes of the input of Ca^{2+} ions.

To conduct a quantitative evaluation of the impact of Fe_3O_4 nanoparticles on the generation of spontaneous contractions, single contraction-relaxation cycles were analyzed by the method of multiparameter mechanokinetic analysis (Kosterin *et al*., 2021). It was determined that under the effect of Fe_3O_4 nanoparticles, other force parameters,

F_C (121.5±1.8 mN and 114.9±2.7 mN, n = 5, p <0.05) and F_R (114.9±2.7 mN (n = 5, p <0.05), increase similarly to the amplitude (**Fig. 6*A***). Against the background of Fe_3O_4, there was also an increase in all time parameters, similar to the force ones, amounting to: time τ_{max} 120.3±3.6 %; τ_C 132.3±4.7 %; τ_R 117.8±4.5 % (in all cases n = 5, p <0.05) (**Fig. 6*B***). Against the background of the nanoparticles, there was also an increase in impulse parameters I_{max}, I_C and I_R, reaching, respectively: 139.8±5.7 %, 160.8±6.2 % and 136.3±7.1 % (**Fig. 6*C***). Contrary to the abovementioned parameters, the indices of the maximal velocities of the contraction and relaxation phases V_C and V_R under the effect of Fe_3O_4 nanoparticles did not differ from the control ones, amounting to, respectively: 96.4±2.8 % and 104.1±5.3 % (n = 5, p >0.05) (**Fig. 6*D***). Therefore, since force and impulse parameters increased, these effects may also be explained by the activation of the processes of the input of Ca^{2+} ions to myocytes under the effect of Fe_3O_4 nanoparticles.

The contractions of circular smooth muscles of the rat *antrum*, induced by the depolarization of the plasma membrane, acetylcholine, and nicotine in the presence of Fe_3O_4 nanoparticles. Since the previous experiments demonstrated the ability of iron oxide nanoparticles to enhance aorta contractions induced by the high-potassium solution (80 mM), we studied similar contractions of smooth muscles of the *antrum*. Similarly to the vascular wall, the preliminary incubation of *antrum* preparations with the suspension of Fe_3O_4 nanoparticles (10^{-4} mg/mL) resulted in a considerable increase in the amplitude of these contractions, on average up to 136.1±8.2 % (n = 5, p <0.05) (**Fig. 7**).

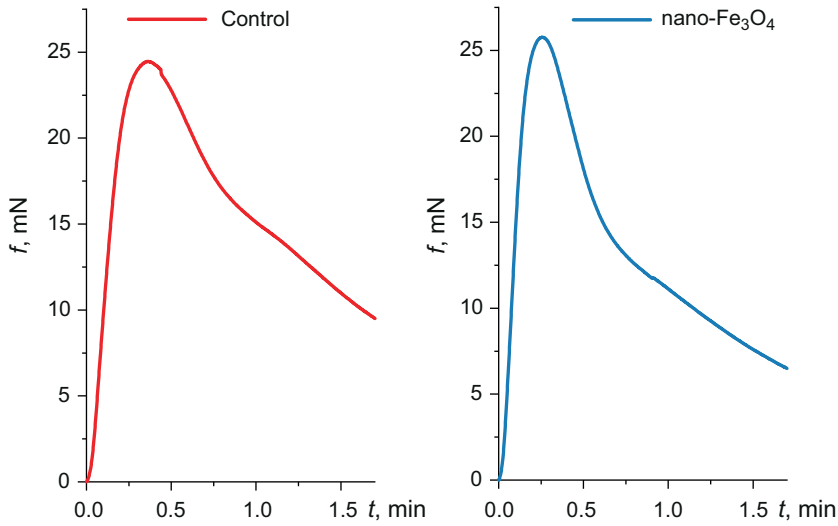

Fig. 7. Typical mechanograms of the contractions of circular smooth muscles of the rat *antrum*, induced by the high-potassium solution (80 mM), in control and under the effect of the suspension of Fe_3O_4 nanoparticles (10^{-4} mg/mL, the duration of the preliminary incubation of 30 min)

The mechanograms of the contractions, activated with the high-potassium solution in control and under the effect of nanoparticles, were analyzed by the mechanokinetic analysis with the evaluation of normalized maximal velocities of contraction and relaxation phases (Burdyga & Kosterin, 1991). A considerable increase in both parameters

was found in the presence of Fe_3O_4: $V_{nc,}$ on average up to 175.9±11.3% (n = 5, p <0.01) and V_{nr}, on average up to 159.6±7.5 % (n = 5, p <0.01).

In the case of both smooth muscles (*antrum* and aorta), the contractile reactions activated by the high-potassium solution are enhanced against the background of Fe_3O_4 nanoparticles. Thus, it may be assumed that voltage-gated Ca^{2+}-channels were activated by Fe_3O_4 nanoparticles in our experiments (Yuan *et al*., 2022). However, since while activating the contractions with the high-potassium solution we did not use the blockers of neuromediator receptors, it may be assumed that the mentioned effects are conditioned by the impact of Fe_3O_4 on the processes of releasing neuromediators (including acetylcholine) or their receptors in the smooth muscle tissue. Acetylcholine is a known key neuromediator in the gastrointestinal tract, and its exogenous application activates both muscarinic receptors in the plasma membrane of myocytes and nicotinic receptors located on postganglionic neurons (Takahashi, 2021). Thus, we studied the contractions of smooth muscles of the *antrum* activated by acetylcholine and nicotine in the presence of Fe_3O_4.

It was found that against the background of Fe_3O_4 there was a considerable increase in the amplitude of acetylcholine-activated contractions (on average up to 137.9±9.1 %, n = 5, p <0.01 regarding the control) (**Fig. 8**). The normalized velocity V_{vc} did not change for these contractions (82.9±11.1 %, n = 5, p >0.05), but there was a considerable increase in V_{nr} (188.36 ± 8.0%, n = 5, p <0.01).

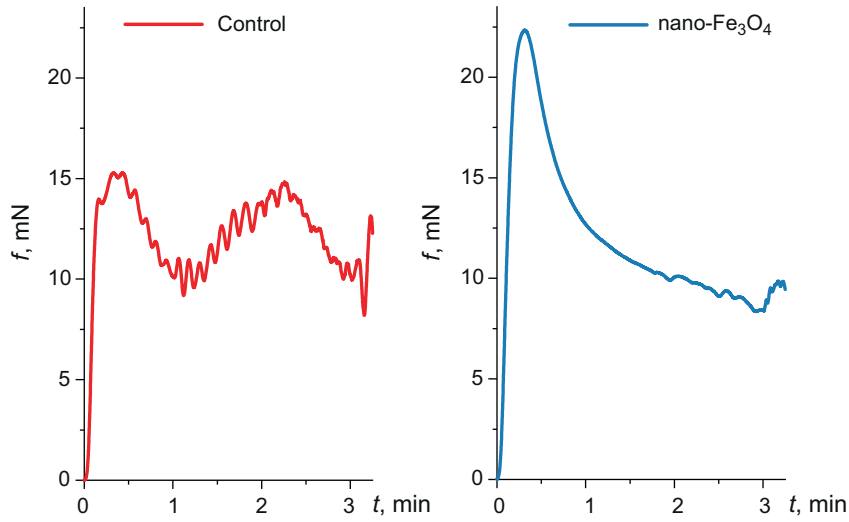

Fig. 8. Typical contractions of circular smooth muscles of the rat *antrum*, induced by acetylcholine (10^{-5} M) in control and under the effect of the suspension of Fe_3O_4 nanoparticles (10^{-4} mg/mL, the duration of the preliminary incubation of 30 min)

The effects of Fe_3O_4 nanoparticles on nicotine-induced contractions were also studied (**Fig. 9**). It was determined that under these conditions, the amplitude of contractions decreased more than four times (21.4 ± 9.6%, n = 5, p<0.001), and there was a considerable increase in the normalized maximal velocities V_{vc} (189.9 ± 17.1%, n = 5, p <0.01) and V_{nr} (149.8 ± 8.7%, n = 5, p <0.05). These effects may be explained by the sorption of nicotine (and catecholamines) with these nanoparticles (Liu *et al*., 2021).

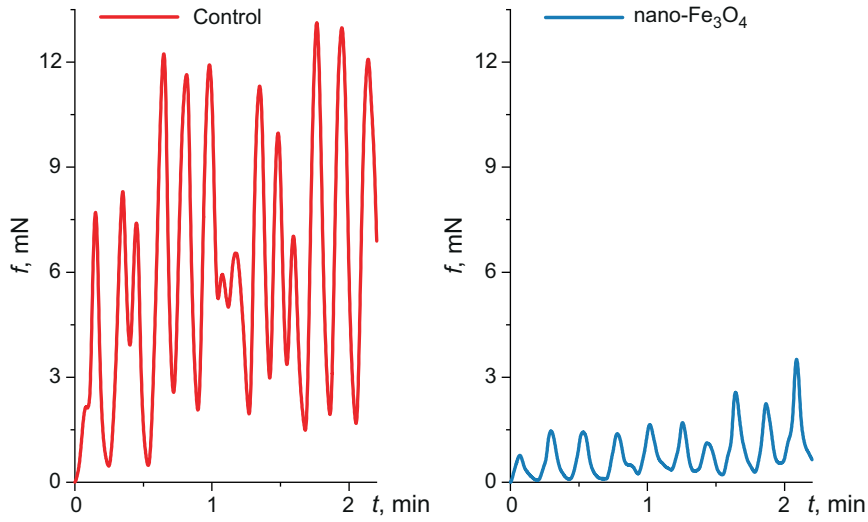

Fig. 9. Typical contractions of the preparations of circular smooth muscles on the rat *antrum* under activation with nicotine (10^{-4} M) in control and under preliminary incubation with Fe_3O_4 nanoparticles (10^{-4} mg/mL)

CONCLUSIONS

The impact of Fe_3O_4 nanoparticles on the functional activity of smooth muscles of the rat aorta and *antrum* was studied in this work. The *in vitro* application of Fe_3O_4 in the concentration of 10^{-4} mg/mL was determined to activate contractions of both muscles, caused by the application of the high-potassium solution. Under the effect of the suspension of Fe_3O_4 nanoparticles, there was a reversible activation of spontaneous contractions in the smooth muscles of the *antrum*. The mechanokinetic analysis demonstrated that Fe_3O_4 caused an increase in force, time, and impulse parameters, likely due to an increase in the intracellular concentration of Ca^{2+} ions in myocytes.

Contrary to the high-potassium contracture, Fe_3O_4 nanoparticles had a multidirectional effect on the contractions of smooth muscles when they were activated by different agonists. For instance, iron oxide caused a considerable inhibition of epinephrine-activated contractions of aorta rings and nicotine-activated contractions of *antrum* preparations, probably due to the sorption of the molecules of these agonists on the surface of the nanoparticles. However, under the effect of Fe_3O_4, there was a considerable increase in acetylcholine-activated contractions of rat *antrum* preparations.

Thus, Fe_3O_4 nanoparticles in the concentration of 10^{-4} mg/mL modulate spontaneous and induced contractions of smooth muscles. The main mechanisms of this modulation may be the activation of voltage-gated input of Ca^{2+} ions to myocytes and sorption of catecholamines with nanoparticles.

COMPLIANCE WITH ETHICAL STANDARDS

Conflict of Interest: the authors declare that they have no conflict of interest.

Human Rights: this article does not contain any studies with human subjects performed by any of the authors.

Animal Studies: all international, national, and institutional guidelines for the care and use of laboratory animals were followed.

AUTHOR CONTRIBUTIONS

Conceptualization, [O.T.; S.K.; Y.P.]; methodology, [Y.P.; O.T.; S.K.; M.I.; D.D.; A.V.; O.C.; O.M.; I.V.]; research, [Y.P.; O.T.; S.K.; O.C.; O.M.; I.V.]; resources, [Y.P.; O.T.; S.K.; M.I.; D.D.; A.V.; O.C.; O.M.; I.V.]; data processing, [Y.P.; O.T.; S.K.; M.I.; D.D.; A.V.; O.C.; O.M.; I.V.]; writing – preparation of the original project, [Y.P.; O.T.; S.K.]; writing – review and editing, [Y.P.; O.T.; S.K.; M.I.; D.D.; A.V.; O.C.; O.M.; I.V.]; visualization, [Y.P.; S.K.; O.T.] supervision, [O.T.; S.K.]; project management, [O.T.; S.K.]; funding search, [–].

All authors have read and agreed to the published version of the manuscript.

REFERENCES

Al-Thani, A. N., Jan, A. G., Abbas, M., Geetha, M., & Sadasivuni, K. K. (2024). Nanoparticles in cancer theragnostic and drug delivery: a comprehensive review. *Life Sciences*, 352, 122899. doi:10.1016/j.lfs.2024.122899
Crossref ● PubMed ● Google Scholar

Angelopoulos, I., Southern, P., Pankhurst, Q. A., & Day, R. M. (2016). Superparamagnetic iron oxide nanoparticles regulate smooth muscle cell phenotype. *Journal of Biomedical Materials Research Part A*, 104(10), 2412–2419. doi:10.1002/jbm.a.35780
Crossref ● PubMed ● PMC ● Google Scholar

Baabu, P. R. S., Kumar, H. K., Gumpu, M. B., Babu K, J., Kulandaisamy, A. J., & Rayappan, J. B. B. (2022). Iron oxide nanoparticles: a review on the province of its compounds, properties and biological applications. *Materials*, 16(1), 59. doi:10.3390/ma16010059
Crossref ● PubMed ● PMC ● Google Scholar

Babsky, A. M., Hekmatyar, S. K., Zhang, H., Solomon, J. L., & Bansal, N. (2005). Application of 23Na MRI to monitor chemotherapeutic response in RIF-1 tumors. *Neoplasia*, 7(7), 658–666. doi:10.1593/neo.05130
Crossref ● PubMed ● PMC ● Google Scholar

Benjamin, A. S., & Nayak, S. (2025). Iron oxide nanoparticles coated with bioactive materials: a viable theragnostic strategy to improve osteosarcoma treatment. *Discover Nano*, 20(1), 18. doi:10.1186/s11671-024-04163-w
Crossref ● PubMed ● PMC ● Google Scholar

Burdyga, T. V., & Kosterin, S. A. (1991). Kinetic analysis of smooth muscle relaxation. *General Physiology and Biophysics*, 10(6), 589–598.
PubMed ● Google Scholar

Capriotti, K., & Capriotti, J. A. (2012). Dimethyl sulfoxide: history, chemistry, and clinical utility in dermatology. *The Journal of Clinical and Aesthetic Dermatology*, 5(9), 24–26.
PubMed ● PMC ● Google Scholar

Castaneda, R. T., Khurana, A., Khan, R., & Daldrup-Link, H. E. (2011). Labeling stem cells with ferumoxytol, an FDA-approved iron oxide nanoparticle. *Journal of Visualized Experiments*, 57, e3482. doi:10.3791/3482
Crossref ● PubMed ● PMC ● Google Scholar

Driscoll, J., Yan, I. K., Angom, R. S., Moirangthem, A., & Patel, T. (2021). Evaluation of *in vivo* toxicity of biological nanoparticles. *Current Protocols*, 1(9), e249. doi:10.1002/cpz1.249
Crossref ● PubMed ● PMC ● Google Scholar

Feng, Q., Liu, Y., Huang, J., Chen, K., Huang, J., & Xiao, K. (2018). Uptake, distribution, clearance, and toxicity of iron oxide nanoparticles with different sizes and coatings. *Scientific Reports*, 8(1), 2082. doi:10.1038/s41598-018-19628-z
Crossref ● PubMed ● PMC ● Google Scholar

Finiuk, N. S., Popovych, M. V., Shalai, Ya. R., Mandzynets, S. M., Grenyukh, V. P., Ostapiuk, Yu. V., Obushak, M. D., Mitina, N. E., Zaichenko, O. S., Stoika, R. S., & Babsky, A. M. (2021). Antineoplastic activity *in vitro* of 2-amino-5-benzylthiazole derivative in complex with nanoscale polymeric carrier. *Cytology and Genetics*, 55(1), 19–27, doi:10.3103/s0095452721010084
Crossref ● Google Scholar

Gholami, A., Rasoul-amini, S., Ebrahiminezhad, A., Seradj, S. H., & Ghasemi, Y. (2015). Lipoamino acid coated superparamagnetic iron oxide nanoparticles concentration and time dependently enhanced growth of human hepatocarcinoma cell line (Hep-G2). *Journal of Nanomaterials*, 2015(1), 451405. doi:10.1155/2015/451405
Crossref ● Google Scholar

Giri, J., Guha Thakurta, S., Bellare, J., Kumar Nigam, A., & Bahadur, D. (2005). Preparation and characterization of phospholipid stabilized uniform sized magnetite nanoparticles. *Journal of Magnetism and Magnetic Materials*, 293(1), 62–68. doi:10.1016/j.jmmm.2005.01.044
Crossref ● Google Scholar

Goud, C., Pitt, B., Webb, R. C., & Richey, J. M. (1998). Synergistic actions of insulin and troglitazone on contractility in endothelium-denuded rat aortic rings. *American Journal of Physiology-Endocrinology and Metabolism*, 275(5), E882–E887. doi:10.1152/ajpendo.1998.275.5.e882
Crossref ● PubMed ● Google Scholar

Hilger, I., Frühauf, S., Linß, W., Hiergeist, R., Andrä, W., Hergt, R., & Kaiser, W. A. (2003). Cytotoxicity of selected magnetic fluids on human adenocarcinoma cells. *Journal of Magnetism and Magnetic Materials*, 261(1–2), 7–12. doi:10.1016/s0304-8853(01)00258-x
Crossref ● Google Scholar

Jia, Z., Song, L., Zang, F., Song, J., Zhang, W., Yan, C., Xie, J., Ma, Z., Ma, M., Teng, G., Gu, N., & Zhang, Y. (2016). Active-target T_1-weighted MR imaging of tiny hepatic tumor *via* RGD modified ultra-small Fe_3O_4 nanoprobes. *Theranostics*, 6(11), 1780–1791. doi:10.7150/thno.14280
Crossref ● PubMed ● PMC ● Google Scholar

Joudeh, N., & Linke, D. (2022). Nanoparticle classification, physicochemical properties, characterization, and applications: a comprehensive review for biologists. *Journal of Nanobiotechnology*, 20(1), 262. doi:10.1186/s12951-022-01477-8
Crossref ● PubMed ● PMC ● Google Scholar

Ju-Nam, Y., Abdussalam-Mohammed, W., & Ojeda, J. J. (2016). Highly stable noble metal nanoparticles dispersible in biocompatible solvents: synthesis of cationic phosphonium gold nanoparticles in water and DMSO. *Faraday Discussions*, 186, 77–93. doi:10.1039/c5fd00131e
Crossref ● PubMed ● Google Scholar

Karim, M., Boikess, R. S., Schwartz, R. A., & Cohen, P. J. (2023). Dimethyl sulfoxide (DMSO): a solvent that may solve selected cutaneous clinical challenges. *Archives of Dermatological Research*, 315(6), 1465–1472. doi:10.1007/s00403-022-02494-1
Crossref ● PubMed ● Google Scholar

Kosterin, S., Tsymbalyuk, O., & Holden, O. (2021). Multiparameter analysis of mechanokinetics of the contractile response of smooth muscles. *Series on Biomechanics*, 35(1), 14–30.
Google Scholar

Lin, T. H., Lu, C. Y., & Tseng, W. L. (2013). Selective enrichment of catecholamines using iron oxide nanoparticles followed by CE with UV detection. *Electrophoresis*, 34(2), 297–303. doi:10.1002/elps.201200285
Crossref ● PubMed ● Google Scholar

Líšková, S., Bališ, P., Mičurová, A., Kluknavský, M., Okuliarová, M., Puzserová, A., Škrátek, M., Sekaj, I., Maňka, J., Valovič, P., & Bernátová, I. (2020). Effect of iron oxide nanoparticles

on vascular function and nitric oxide production in acute stress-exposed rats. *Physiological Research*, 69(6), 1067–1083. doi:10.33549/physiolres.934567
Crossref ● PubMed ● PMC ● Google Scholar

Liu, J., Ji, C., Liu, X., Li, X., Wu, H., & Zeng, D. (2021). Fe_3O_4 nanoparticles as matrix solid-phase dispersion extraction adsorbents for the analysis of thirty pesticides in vegetables by ultrahigh-performance liquid chromatography-tandem mass spectrometry. *Journal of Chromatography B*, 1165, 122532. doi:10.1016/j.jchromb.2021.122532
Crossref ● PubMed ● Google Scholar

Mashouf, P., Tabibzadeh, N., Kuraoka, S., Oishi, H., & Morizane, R. (2024). Cryopreservation of human kidney organoids. *Cellular and Molecular Life Sciences*, 81(1), 306. doi:10.1007/s00018-024-05352-7
Crossref ● PubMed ● PMC ● Google Scholar

Mehta, K. J. (2022). Iron oxide nanoparticles in mesenchymal stem cell detection and therapy. *Stem Cell Reviews and Reports*, 18(7), 2234–2261. doi:10.1007/s12015-022-10343-x
Crossref ● PubMed ● PMC ● Google Scholar

Nowak-Jary, J., & Machnicka, B. (2024). Comprehensive analysis of the potential toxicity of magnetic iron oxide nanoparticles for medical applications: cellular mechanisms and systemic effects. *International Journal of Molecular Sciences*, 25(22), 12013. doi:10.3390/ijms252212013
Crossref ● PubMed ● PMC ● Google Scholar

Obireddy, S. R., & Lai, W.-F. (2022). ROS-generating amine-functionalized magnetic nanoparticles coupled with carboxymethyl chitosan for pH-responsive release of doxorubicin. *International Journal of Nanomedicine*, 17, 589–601. doi:10.2147/ijn.s338897
Crossref ● PubMed ● PMC ● Google Scholar

Olsen, T. R., Mattix, B., Casco, M., Herbst, A., Williams, C., Tarasidis, A., Simionescu, D., Visconti, R. P., & Alexis, F. (2015). Manipulation of cellular spheroid composition and the effects on vascular tissue fusion. *Acta Biomaterialia*, 13, 188–198. doi:10.1016/j.actbio.2014.11.024
Crossref ● PubMed ● PMC ● Google Scholar

Ramnarine, S. I., Hirayama, Y., Barnes, P. J., & Rogers, D. F. (1994). 'Sensory-efferent' neural control of mucus secretion: characterization using tachykinin receptor antagonists in ferret trachea *in vitro*. *British Journal of Pharmacology*, 113(4), 1183–1190. doi:10.1111/j.1476-5381.1994.tb17122.x
Crossref ● PubMed ● PMC ● Google Scholar

Rivière, C., Boudghène, F. P., Gazeau, F., Roger, J., Pons, J. N., Laissy, J. P., Allaire, E., Michel, J. B., Letourneur, D., & Deux, J. F. (2005). Iron oxide nanoparticle-labeled rat smooth muscle cells: cardiac MR imaging for cell graft monitoring and quantitation. *Radiology*, 235(3), 959–967. doi:10.1148/radiol.2353032057
Crossref ● PubMed ● Google Scholar

Salimi, M., Mosca, S., Gardner, B., Palombo, F., Matousek, P., & Stone, N. (2022). Nanoparticle-mediated photothermal therapy limitation in clinical applications regarding pain management. *Nanomaterials*, 12(6), 922. doi:10.3390/nano12060922
Crossref ● PubMed ● PMC ● Google Scholar

Shi, N., Bu, X., Zhang, M., Wang, B., Xu, X., Shi, X., Hussain, D., Xu, X., & Chen, D. (2022). Current sample preparation methodologies for determination of catecholamines and their metabolites. *Molecules*, 27(9), 2702. doi:10.3390/molecules27092702
Crossref ● PubMed ● PMC ● Google Scholar

Shoudho, K. N., Uddin, S., Rumon, M. M. H., & Shakil, M. S. (2024). Influence of physicochemical properties of iron oxide nanoparticles on their antibacterial activity. *ACS Omega*, 9(31), 33303–33334. doi:10.1021/acsomega.4c02822
Crossref ● PubMed ● PMC ● Google Scholar

Shukla, S., Jadaun, A., Arora, V., Sinha, R. K., Biyani, N., & Jain, V. K. (2015). *In vitro* toxicity assessment of chitosan oligosaccharide coated iron oxide nanoparticles. *Toxicology Reports*, 2, 27–39. doi:10.1016/j.toxrep.2014.11.002
Crossref ● PubMed ● PMC ● Google Scholar

Singh, R., Yadav, D., Ingole, P. G., & Ahn, Y.-H. (2024). Magnetic engineering nanoparticles: versatile tools revolutionizing biomedical applications. *Biomaterials Advances*, 163, 213948. doi:10.1016/j.bioadv.2024.213948
Crossref ● PubMed ● Google Scholar

Subotin, V. V., Ivanytsya, M. O., Terebilenko, A. V., Yaremov, P. S., Pariiska, O. O., Akimov, Y. M., Kotenko, I. E., Sabov, T. M., Kurmach, M. M., Ryabukhin, S. V., Volochnyuk, D. M., & Kolotilov, S. V. (2023). Air-stable efficient nickel catalyst for hydrogenation of organic compounds. *Catalysts*, 13(4), 706. doi:10.3390/catal13040706
Crossref ● Google Scholar

Takahashi, T. (2021). Multiple roles for cholinergic signaling from the perspective of stem cell function. *International Journal of Molecular Sciences*, 22(2), 666. doi:10.3390/ijms22020666
Crossref ● PubMed ● PMC ● Google Scholar

Vakili-Ghartavol, R., Momtazi-Borojeni, A. A., Vakili-Ghartavol, Z., Aiyelabegan, H. T., Jaafari, M. R., Rezayat, S. M., & Arbabi Bidgoli, S. (2020). Toxicity assessment of superparamagnetic iron oxide nanoparticles in different tissues. *Artificial Cells, Nanomedicine, and Biotechnology*, 48(1), 443–451. doi:10.1080/21691401.2019.1709855
Crossref ● PubMed ● Google Scholar

Vallabani, N. V. S., & Singh, S. (2018). Recent advances and future prospects of iron oxide nanoparticles in biomedicine and diagnostics. *3 Biotech*, 8(6), 279. doi:10.1007/s13205-018-1286-z
Crossref ● PubMed ● PMC ● Google Scholar

Vukova, T. I., Dimitrov, S. D., Gagov, H. S., & Dimitrova, D. Z. (2016). In focus: Fe_3O_4 nanoparticles and human mesenteric artery interaction *in vitro*. *Nanomedicine*, 11(8), 921–932. doi:10.2217/nnm.16.25
Crossref ● PubMed ● Google Scholar

Wang, H., Zhao, B., Huang, L., Zhu, X., Li, N., Huang, C., Han, Z., & Ouyang, K. (2025). Conditional deletion of IP_3R1 by Islet1-Cre in mice reveals a critical role of IP_3R1 in interstitial cells of Cajal in regulating GI motility. *Journal of Gastroenterology*, 60(2), 152–165. doi:10.1007/s00535-024-02164-1
Crossref ● PubMed ● Google Scholar

Wang, Y., Li, B., Xu, H., Du, S., Liu, T., Ren, J., Zhang, J., Zhang, H., Liu, Y., & Lu, L. (2020). Growth and elongation of axons through mechanical tension mediated by fluorescent-magnetic bifunctional Fe_3O_4·Rhodamine 6G@PDA superparticles. *Journal of Nanobiotechnology*, 18(1), 64. doi:10.1186/s12951-020-00621-6
Crossref ● PubMed ● PMC ● Google Scholar

Wu, L., Wen, W., Wang, X., Huang, D., Cao, J., Qi, X., & Shen, S. (2022). Ultrasmall iron oxide nanoparticles cause significant toxicity by specifically inducing acute oxidative stress to multiple organs. *Particle and Fibre Toxicology*, 19(1), 24. doi:10.1186/s12989-022-00465-y
Crossref ● PubMed ● PMC ● Google Scholar

Yan, J., Li, S., Cartieri, F., Wang, Z., Hitchens, T. K., Leonardo, J., Averick, S. E., & Matyjaszewski, K. (2018). Iron oxide nanoparticles with grafted polymeric analogue of dimethyl sulfoxide as potential magnetic resonance imaging contrast agents. *ACS Applied Materials & Interfaces*, 10(26), 21901–21908. doi:10.1021/acsami.8b06416
Crossref ● PubMed ● Google Scholar

Yang, L., Kuang, H., Zhang, W., Aguilar, Z. P., Xiong, Y., Lai, W., Xu, H., & Wei, H. (2015). Size dependent biodistribution and toxicokinetics of iron oxide magnetic nanoparticles in mice. *Nanoscale*, 7(2), 625–636. doi:10.1039/c4nr05061d
Crossref ● PubMed ● Google Scholar

Yang, H. Y., Steenhuis, P., Glucksman, A. M., Gurenko, Z., La, T. D., & Isseroff, R. R. (2021). Alpha and beta adrenergic receptors modulate keratinocyte migration. *PloS One*, 16(7), e0253139. doi:10.1371/journal.pone.0253139
Crossref ● PubMed ● PMC ● Google Scholar

Yoneda, S., Fukui, H., & Takaki, M. (2004). Pacemaker activity from submucosal interstitial cells of Cajal drives high-frequency and low-amplitude circular muscle contractions in the mouse proximal colon. *Neurogastroenterology and Motility*, 16(5), 621–627. doi:10.1111/j.1365-2982.2004.00546.x
Crossref ● PubMed ● Google Scholar

Yotsomnuk, P., Skolpap, W., & Thitapakorn, V. (2025). Release dynamics and toxicological analysis of astilbin from lauric acid/BSA-coated superparamagnetic iron oxide nanoparticles. *Colloids and Surfaces. B, Biointerfaces*, 252, 114620. doi:10.1016/j.colsurfb.2025.114620
Crossref ● PubMed ● Google Scholar

Younis, N. K., Roumieh, R., Bassil, E. P., Ghoubaira, J. A., Kobeissy, F., & Eid, A. H. (2022). Nanoparticles: attractive tools to treat colorectal cancer. *Seminars in Cancer Biology*, 86(2), 1–13. doi:10.1016/j.semcancer.2022.08.006
Crossref ● PubMed ● Google Scholar

Yuan, M., Bancroft, E. A., Chen, J., Srinivasan, R., & Wang, Y. (2022). Magnetic fields and magnetically stimulated gold-coated superparamagnetic iron oxide nanoparticles differentially modulate L-type voltage-gated calcium channel activity in midbrain neurons. *ACS Applied Nano Materials*, 5(1), 205–215. doi:10.1021/acsanm.1c02665
Crossref ● PubMed ● PMC ● Google Scholar

Zhang, W., Gao, J., Lu, L., Bold, T., Li, X., Wang, S., Chang, Z., Chen, J., Kong, X., Zheng, Y., Zhang, M., & Tang, J. (2021). Intracellular GSH/GST antioxidants system change as an earlier biomarker for toxicity evaluation of iron oxide nanoparticles. *NanoImpact*, 23, 100338. doi:10.1016/j.impact.2021.100338
Crossref ● PubMed ● Google Scholar

Zhao, S., Yu, X., Qian, Y., Chen, W., & Shen, J. (2020). Multifunctional magnetic iron oxide nanoparticles: an advanced platform for cancer theranostics. *Theranostics*, 10(14), 6278–6309. doi:10.7150/thno.42564
Crossref ● PubMed ● PMC ● Google Scholar

ВПЛИВ *IN VITRO* НАНОЧАСТИНОК Fe_3O_4 НА СКОРОЧУВАЛЬНУ АКТИВНІСТЬ ГЛАДЕНЬКИХ М'ЯЗІВ *ANTRUM* І АОРТИ ЩУРІВ

***Юлія Подгаєцька*[1], *Сергій Колотілов*[2], *Микита Іваниця*[2,4], *Діана Дороніна*[2,4], *Анна Вельбовець*[4], *Олександр Чуніхін*[3], *Оксана Маланчук*[5], *Іван Войтешенко*[1], *Ольга Цимбалюк*[1]**

[1] *Київський національний університет імені Тараса Шевченка вул. Володимирська,64/13, Київ 01601, Україна*

[2] *Інститут фізичної хімії ім. Л. В. Писаржевського НАН України просп. Науки, 31, Київ 03028, Україна*

[3] *Інститут біохімії ім. О. В. Палладіна НАН України, вул. Леонтовича, 9, Київ 01601, Україна*

[4] *ТОВ НВП "Єнамін", вул. Вінстона Черчилля, 78, Київ 02094, Україна*

[5] *Львівський національний медичний університет імені Данила Галицького вул. Пекарська, 69, Львів 79010, Україна*

Обґрунтування. Магнітні наночастинки оксиду заліза є одними з найбільш перспективних матеріалів для створення на їхній основі новітніх засобів тераностики злоякісних новоутворень. На сьогодні впроваджено в діагностичну і лікарську практику низку медичних препаратів на основі наночастинок оксиду заліза, які застосовують у МРТ діагностиці й фоточутливій терапії, а також як джерело заліза для хворих на дефіцит цього елемента. Втім, ці наночастинки не є повністю нейтральними щодо функцій органів і тканин організму, зокрема, серцево-судинної, дихальної, сечостатевої та центральної нервової систем. Оскільки дія наночастинок Fe_3O_4 на скорочення гладеньких м'язів шлунково-кишкового тракту і аорти не є дослідженою, метою було з'ясувати закономірності й механізми впливу за дії *in vitro* цих наночастинок на функціональну активність кільцевих гладеньких м'язів шлунку та препаратів кілець аорти щурів.

Матеріали і методи. У дослідженнях використовували суспензію наночастинок Fe_3O_4. Середній гідродинамічний діаметр наночастинок Fe_3O_4 у суспензії за використання стабілізації олеїновою кислотою (1%), бичачим сироватковим альбуміном (7,5%) та ДМСО (1%) визначали методом динамічного розсіювання світла.

Тензометричні досліди проводили в ізометричному режимі реєстрації на ізольованих препаратах кільцевих гладеньких м'язів антрального відділу шлунку і кілець грудної аорти щурів. У дослідженні м'язів шлунку скорочення індукували аплікуванням гіперкалієвого розчину (80 мМ), ацетилхоліну (10^{-5} М) і нікотину (10^{-4} М), а у дослідженні препаратів аорти – гіперкалієвим розчином (80 мМ) та епінефрином (10^{-6} М). Скорочення аналізували методами механокінетичного аналізу.

Результати. Встановлено, що за умов використання ДМСО як стабілізатора суспензія містила мінімальну кількість агрегатів наночастинок Fe_3O_4 та характеризувалася піком частинок зі середнім значенням 67,2 нм і шириною 75,3 нм (за кількістю) та була досить стабільною. Встановлено, що застосування *in vitro* Fe_3O_4 (10^{-4} мг/мл) спричиняє активацію викликаних аплікуванням гіперкалієвого розчину скорочень гладеньком'язових препаратів шлунку й аорти. Також за дії Fe_3O_4 спостерігали оборотну активацію спонтанних скорочень гладеньких м'язів шлунку; механокінетичним аналізом встановлено, що Fe_3O_4 спричиняє зростання їхніх силових, часових та імпульсних параметрів.

Виявлено, що за дії наночастинок Fe_3O_4 суттєво зменшуються епінефрин-активовані скорочення кілець аорти і нікотин-активовані скорочення препаратів шлунку. Однак Fe_3O_4 спричиняє суттєве підсилення ацетилхолін-активованих скорочень препаратів шлунку.

Висновки. Наночастинки Fe_3O_4 модулюють спонтанні та викликані скорочення гладеньких м'язів антрального відділу шлунку й аорти. Головними механізмами такої модуляції є, ймовірно, активація потенціалкерованого надходження іонів Ca^{2+} до гляденьком'язових клітин і сорбція цими наночастинками епінефину та нікотину.

Ключові слова: аорта, антральний відділ шлунку, наночастинки Fe_3O_4, потенціалкеровані Ca^{2+}-канали, ацетилхолін, епінефрин, нікотин, механокінетичні параметри

Received / Одержано 04 July, 2025 | Revision / Доопрацьовано 26 August, 2025 | Accepted / Прийнято 17 September, 2025 | Published / Опубліковано 24 September, 2025